Volumetric design for ORC-VCC compressor-expander units.

Michaël Marion, Hasna Louahlia

Volumetric design for ORC-VCC compressor-expander units.

Michaël MARION*, Hasna LOUAHLIA
Normandie Univ, UNICAEN, LUSAC-EA 4253, F-50000 Saint-Lô, France

* Corresponding author: Michaël Marion
Tel : +33 233771163 (M. M.)
Fax : +33 233771178
e-mail : michael.marion@unicaen.fr

ABSTRACT
The combination of an ORC (Organic Rankine Cycle) with a VCC (Vapor Compression Cycle) is studied analytically. In this work, the two cycles use the same fluid and operate with a common condenser. Elementary transformations of the fluid between two consecutive points of the system are calculated using a one-dimensional thermodynamic approach considering real fluid properties, the pressure losses and irreversibilities present in the compressor, in the expander and in the pump. The performances and the recommended inlet and outlet diameters of the expander and the compressor are established for various operating conditions and 12 fluids. The system can produce a typical useful cooling capacity of 0.60 kW at 5.5 °C when using a 2 kW heating source at 65 °C and when the condenser temperature is 30 °C. The cooling capacity reaches 1.0 kW if the cold source temperature is 15.5 °C. Results show the required diameters ratios at inputs and outputs of the compressor and the expander. They indicate the situations for which the compressor is smaller than the expander and vice versa. They identify the particular cases in which the compressor and the expander have exactly the same inlet and outlet diameters. This particular case allows using two identical compressors, one working as a compressor, the second as an expander.

Keywords: refrigeration, ORC, Rankine cycle, heat powered cooling, energetic efficiency.

NOMENCLATURE

Symbols	
D	diameter, (m)
H	enthalpy, (kJ.kg^{-1})
L	Length, (m)
$\dot{m}$	mass flow, (kg.s^{-1})
P	Pressure (Pa)
T	Temperature, (K)
v	Velocity, (m.s^{-1})
V	Volume flow rate, (m^3.s^{-1})
$\dot{W}$	mechanical power, (kW)
ρ	density, (kg.m^{-3})
η	efficiency
Λ	friction coefficient

Subscripts	
c	compressor
cond	condenser
e	expander
ev	evaporator
gen	generator
i	point number
is	isentropic
j	point number
m	mechanical
p	primary
pre	preheater
s	secondary

1. Introduction

The electric power consumption increases years after years during summers for air conditioning applications. Therefore, heat powered cooling systems benefit recently from renewed interest due to needs to reduce electric consumption for cooling application and great advancements in Organic Rankine Cycles (ORC). Started with the first oil shock, powering a cooling system thanks solar heat, geothermal heat or waste heat has been the subject of numerous studies. Zeghami et al. (2015) present a review of recent and past works on solar

thermo-mechanical refrigeration and cooling methods. The absorption or ejection cycle systems have shown their possibilities but also their limitations, especially that of not allowing the use of heating sources as low as 60-90 °C. Wang et al. (2020) carried out thermal, economic and environmental analysis of an ORC - CCHP system powered by biomass at the domestic scale for a Chinese climate. The system contains R134a, Dimethyl formyl and Helium and uses diffusion absorption refrigeration cycle. Their results show that energetic system efficiency is about 55 % and CO_2 emission reduction is 0.15 tons. Vapor compression cycle (VCC) powered by ORC has many advantages, as they can produce an important part of the cold needs from natural sources or thermal discharges which, anyway, would have been lost. Habibzadeh et al. (2013) have studied combination of an ejector refrigeration cycle with an ORC cycle thermodynamically. The shaft mechanical power is transformed into electricity and the optimum situation giving the smallest thermal conductance and exergy destruction is obtained with R601a. Nasir et al. (2019) studied a system combining an Organic Rankine Cycle with a Vapor Compression Cycle (ORC-VCC) for air-conditioning applications. The authors investigate first and second laws efficiencies for R245fa, R600, R600a, and R134a combinations. R600a for ORC and R245fa for VCC was found to be the better one.

Aphornratana and Sriveerakul (2010) analyzed that ORC-VCC unit can run correctly, when the low-grade heating source temperature is 60-95°C and the cooling temperature is ±10°C. Using R22 and R134a, the two subsystems are connected thanks a free linear piston running as an expander-compression unit. The predicted global COP varies from 0.1 to 0.6. ORC-VCC have been also the subject of theoretical and experimental studies concerning the choice of the fluid (Zheng et al., 2018; Molés et al., 2015; Nasir and Kim. 2016), the architecture of the system (Zeyghami et al., 2015), the operating temperatures (Karellas and Braimakis, 2016; Marion and Louahlia, 2017; Li et al., 2013), or combination thereof (Kim and Perez-Blanco, 2015; Saleh, 2016; Lizarte et al., 2017) to assess the system energetic, exergetic or economic performances. The ORC-VCC systems can use the same fluid, which makes it possible to use a common condenser (Marion and Louahlia, 2017; Li et al., 2013; Saleh, 2016; Lizarte et al., 2017). They can use different fluids and then offer the possibility of producing electricity when cold production is not needed (Wu et al., 2017; Molés et al, 2015; Karellas and Braimakis, 2016). In this case, a strong sealing is required for the rotation shafts of the compressor and the expander that reduces the efficiency of the mechanical coupling.

Small-scale systems (~kW cooling power) are also studied because they can be used for domestic applications (Chang et al., 2017; Muhammad et al, 2015) or for vehicle air conditioning (Yue et al., 2016; Wang et al, 2011). For example, Wang et al. (2011) measured a COP closed to 0.5 when operating a 5 kW cooling capacity unit using scroll technology for expender and compressor. To minimize seal frictional losses, the authors used a compliant scroll design with minimized shaft diameter to reduce the shaft seal friction by reducing the interface. One can note that few studies deal with the small-scale direct mechanical coupling of an ORC with VCC. Expanders are not available and very often, the compressors are hermetic type. Researchers are therefore required to manufacture their own expander or to adapt existing elements (Demierre et al., 2014; Pu et al., 2016). Due to the lack of availability of small-scale expanders, Quolin et al. (2010) test successfully a scroll compressor working as an expander in small-scale ORC systems. Zheng et al. (2013) calculated the performance of various HCs-HFO-HFCs zeotropic mixtures for solar powered ORC-VCC refrigeration. The highest efficiency predicted is 0.3089 when the system operates when the cold and the hot sources temperatures are respectively -5 and 80°C. Li et al. (2017) report first tests results from a prototype. A very small ORC efficiency (1%) is obtained when using small-scale ORC unit utilizing low-grade heat source. However, Bracco et al. (2015) measured about 8% efficiency with domestic-scale ORC prototype. Nasir and Kim (2016) present the thermal performance of an ORC-VCC

separated system when combining R245fa, R123, R134a, R1234yf, R1234ze (E), Butane and Isobutane when 100°C water is used as heating source. Using isentropic efficiencies for pump, compressor and expander equal to 80%, they found that ORC (R134a) + VCC (Isobutane) correspond to the best combination. When the system is designed for air conditioning application, they established that ORC efficiency is typically 4.5-6 %, the VCC COP is 3.5-4.8 making the overall thermal performance close to 21.6 %. Jeong and Kang (2004) analyzed an ORC-VCC system using a common fluid and a common condenser when the temperature of the heating source is 220-230 °C. The performance increases by 47 % when adding a regenerator. The highest thermal efficiency is 1.75. Bao et al. (2020) studied the combined ORC-VCC system when using single and dual fluid systems. The VCC cycle was single stage or used the flash tank vapor injection cycle. The heating source is geothermal water (100-150°C). The authors obtained cops of the order of 0.4 and show that the best combination is obtained when the ORC fluid is different from the VCC fluid.

Emerging from these studies, the required mass flow rate in the ORC to produce the desired masse flow rate in the VCC constitutes an important element that must be considered when one wants to design a new system. The lower the required ORC mass flow rate, the higher the performance, and vice versa. The direct mechanical shaft coupling of the expander and the compressor rotors in a closed housing allows reducing the compressor and expander shaft sealing that reduces the friction, which are proportionally greater for small systems. However, this solution requires using the same fluid for the ORC and the VCC, which makes it possible to use a common condenser. The literature (Marion and Louahlia, 2017; Li et al., 2013; Kim and Perez-Blanco, 2015; Saleh, 2016; Yilmaz, 2015) indicates that this solution has already been tested with promising results and that it therefore seems suitable for small-scale applications such as individual air conditioning. In this work, the performance and required diameters at inlet and outlet of the compressor and expander are established for various operating conditions and for a variety of twelve fluids.

2. Description and modeling of the cooling system

2.1. System description

The ORC system consists of a generator, an expander, a condenser and a pump. The VCC system completes the previous one with a pressure reducer, an evaporator and a compressor. The assembly is presented in Fig. 1.

The ORC vapor flow is produced in the generator (4) and goes into the volumetric expender to produce mechanical work during expansion process (5). The recovered mechanical work directly drives a volumetric compressor extracting the secondary vapor flow from the evaporator (12). The flows leaving the expender and the compressor mixed at the same pressure (7) and flow through the preheater (8) and then through the condenser where phase change occurs. A fraction of the liquid outgoing from the condenser (9) is pumped (1) to the preheater (2) and to the vapor generator (3) completing the ORC. The rest of the liquid flows through the pressure-reducer (10) and returns to the evaporator (11) where it produces the useful cooling effect and completes the VCC.

Conventional components such as the condenser, expansion valve or evaporators are mature technologies that are widely available in the refrigeration machine or air conditioner market. Only the coupled expander - compressor unit is not mature and constitutes a lock for the development of this system.

Thermodynamic coefficients VFR and SP are usually used to assess the expander size (Kim and Perez-Blanco, 2015). VFR is the isentropic volumetric flow ratio and is defined as : $VFR = \frac{V_{5\,is}}{V_4}$, where subscript *5is* designed the specific enthalpy at expander outlet calculated for an isentropic expander. Small values of VFR is preferred to expect expansion close to reversible transformation.

SP is the isentropic volumetric flow ratio and is defined by : $SP = \frac{\sqrt{V_{5\,is}}}{\sqrt[4]{(h_{5\,is} - h_4)}}$.

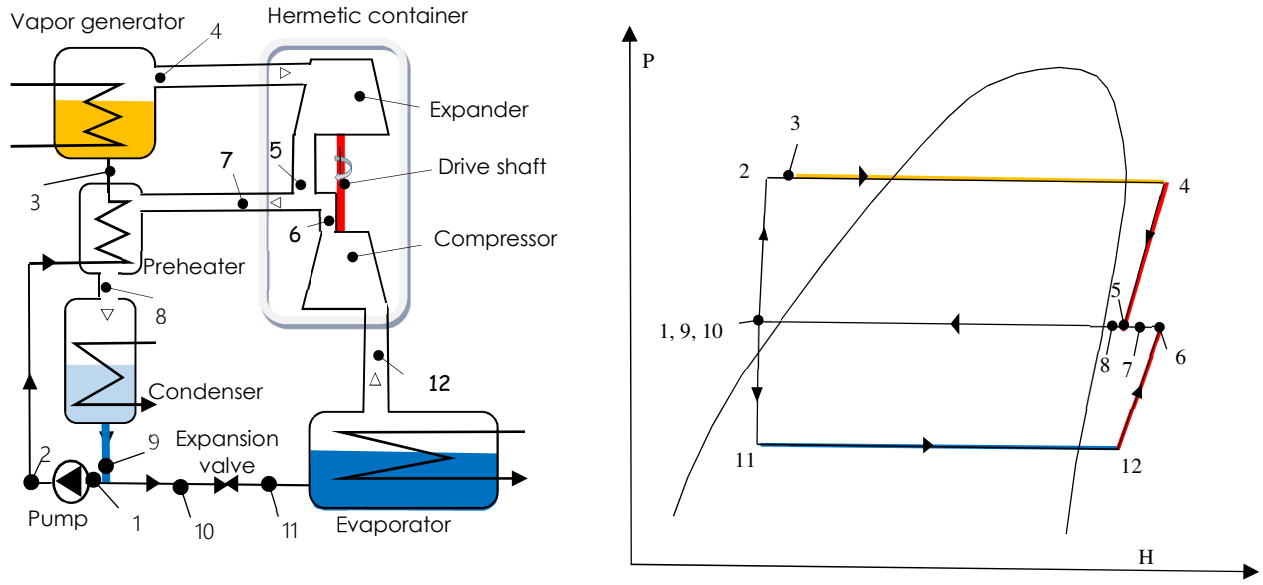

Fig. 1. Description of the ORC-VCC system and corresponding P-H diagram.

Similarly, small SP value indicates that the work density production is high which means that smallest expander is required.

In this work, the shaft of the compressor is directly connected with that of the expander in a hermetic box. This imposes the same rotational speed for the compressor and the expander. It is therefore also necessary to correctly size the two devices. The advantage lies in the mechanical simplicity of the solution and in not communicating any rotating part with the outside, thus producing less friction

In the present work, the expected sizes of the compressor and the expander are analyzed. In particular, their individual volumetric characteristics are evaluated in order to identify whether the compressor should be smaller or larger than the expander and whether the volumetric compression ratio should be greater or smaller than the volumetric expansion rate. Thus, the volumetric ratios at the inlet and outlet of the compressor and expander are carefully reviewed.

2.2. Cycle modeling

The complete system is modeled by a one-dimensional thermodynamic approach. Details of model equations are presented in (Marion and Louahlia, 2017) and main equations are presented in appendix. The model is based on the thermodynamic analysis applied to each individual element. It is established for stationary conditions; the kinetic and gravitational energies are neglected. The shaft work produced by the expander is equal to the shaft work consumed by

the compressor and the shaft mechanical friction losses. The latter are considered equal to 5% of the work of the expander. The mass flow rates calculated in the ORC and VCC cycles are adjusted iteratively until the power of the boiler is equal to that of the hot source (2 kW). Hydraulic efficiency of the pump, pressure drops in the individual components and non-isentropic transformations in the expander and the compressor are considered. Fluid properties are established at the input and output of each component using the NIST REFPROP software (2010). The selected velocity in pipes is 1 m/s when the fluid is in liquid state and 5 m/s when it is in vapor state. The pressure drops are calculated between two consecutive points i and j assuming lengths equivalent corresponding to typical lengths observed on existing cooling systems of similar powers. Selected equivalent lengths for sections with phase change (3-4 ; 8-9; 11-12), is 5 m. Selected equivalent lengths for sections without phase change (2-3; 7-8; 9-1; 9-10), is 0.5 m.

After selecting the fluid, required data to run the thermodynamic model are the evaporator cold source inlet temperature and the cooling flow temperature entering in the condenser.
The model calculates fluid properties and flows rates of individual points of the system and the corresponding required diameters. The thermal powers of the evaporator, condenser and regenerator and the mechanical shaft powers of the pump, expander and compressor are calculated.

2.3. Selection of working parameters

Since the system considers fixed volumetric vane expander and compressor, the expansion and compression ratios are of prime importance to prevent the system running when under/over expansion or compression occurs. Under/over expansion occurs if the actual operating volume ratio of the expander is lower/greater than the designed volume ratio. The ratio of the operating volume required at inlet and outlet of the expander depends on the inlet temperature and pressure ratio. The last parameter depends on the temperature phase change fixed in the generator and the condenser. Likewise, insufficient / excessive compression occurs when the compressor operating volume ratio is lower / higher than the designed operating volume ratio. The operating volume ratio of the compressor depends on the compressor inlet temperature and the compressor pressure ratio. The last parameter depends on the temperature phase change fixed in the evaporator and the condenser. In this study, the condensation temperature varies from 20 to 40 °C. Domestic air conditioning application correspond to the highest temperatures because the condenser is usually cooled by outside air whose temperature is naturally high when air conditioning is required. Extension of the system for other potential application is also investigated. The condensation temperatures close to 20 °C and the evaporator at 0.5 ° C correspond to this type of situation.

The power of the vapor generator is fixed (=2 kW) and the inlet temperature of hot source is 65 °C. A reasonable overheating/ sub cooling equal to 4 ° C is set for the working fluid at the outlet of the boiler, evaporator and condenser. A temperature difference equal to 5 °C is set in the generator, the condenser and the evaporator, between the input of the source temperature and the phase change the temperature. The preheater efficiency is 85%. Isentropic pump and compressor efficiencies are 85%. Expander isentropic efficiency is only 50% or 70%. The first value corresponds to the experimental value measured on our small-scale system (Marion and Louahlia, 2017). The second one corresponds to the measured value on a spiral expander by Wang et al. (2011). According to authors, the values ranging from 70% to 84% depends on the fixed pressure rates, but confirm that such values can be achieved when using a small-scale ORC-VCC combined system. Sensitivity analysis has been conducted to measure the effect of the condenser and evaporator temperatures on the performance and volumetric flow rates.

2.3. Selection of the working fluids

The choice of fluids should consider physical properties such as density, latent heat of vaporization, and operating pressures. These characteristics influence the size of the components and therefore the compactness and cost of the system. The choice of fluids should also consider existing and future regulations on refrigerants that aim to ban fluids with high GWP. In this work, 12 pure fluids were selected from hydrofluoroolefins (HFOs), hydrofluorocarbons (HFCs), hydrocarbons (HCs) and alcohol that have been already used for VCC and ORC systems. Some fluids with high GWP were kept in the selection. This choice makes it possible to preserve a wide range of NBP.

Table 1 Properties of selected fluids.

Name	NBP (°C)	GWP_{100y}	Classification	type
R125	-48.3	3170	A1	wet
R1270	-47.9	3	A3	wet
R290	-42.1	20	A3	wet
R1234yf	-29.8	4	A2	dry
R134a	-26.1	1300	A1	wet
R227ea	-16.6	3350	A1	dry
R236fa	-1.44	9810	A1	isentr.
R600	-0.5	20	A3	dry
R245fa	15.1	858	B1	dry
R601a	27.4	5	A3	dry
R365mfc	4.2	804	A2	dry
methanol	64.7	3	A3	wet

Table 1 resumes the main properties of the 12 selected fluids. Wet or dry type fluids have been selected. A fluid is classified “wet” when the isentropic line enters the two-phase zone during relaxation. A fluid is classified as dry or isentropic when the isentropic moves away or remains parallel to the two-phase zone during expansion. Whatever the fluid tested, no simulation predicts liquid formation during expansion process. This is due to the selected reasonably low value of isentropic expansion efficiency and sufficient overheating of the boiler outlet.

3 Results and discussion

3.1. System performance

The coefficient of performance COP corresponds to the ratio between the cooling power produced at the evaporator and the thermal power consumed in the generator (=2kW). It is presented in Fig. 2 as a function of the condensation temperature, for each fluid studied and for all physical values tested. The calculations predict low but acceptable COP.

We can observe in Fig. 2a that COP vary for all the fluids studied from 0.2 to 0.6. It essentially depends on the condensing temperature. These values can be compared with those obtained with other refrigeration systems such as absorption and ejection machines.
One can note that first one requires at least a 100°C heating source to operate and many studies deal with ejection cycles but this second system is currently underdeveloped for small units. Using R245fa as working fluid, the typical measured COP by Eames et al. (2013) is about 0.15

when the evaporating temperature of the 40 kW ejector chiller is 10 °C, the condensing temperature is 32 °C, and the generator temperature is 110 °C. According to Mazzelli and Milazzo (2015), the predicted and measured COP for a supersonic ejector system powered by a 90-100 °C thermal source is close to 0.4-0.6. This value is close to the performance of single-effect absorption systems.

The performances predicted in the present study when using hydrocarbons in ORC cooling cycles are similar to those already obtained by Tchanche et al. (1990) with ORC or Habibzadeh et al. (2013) with ejection cycles. The same trend is observed by Wang et al. (2016).

As can be observed on Fig. 2b, 2c and 2d, COP increases when increasing the temperature of the evaporator and increasing the efficiency of the expander.

Comparing Fig. 2a) and 2c) with Fig. 2b) and 2d), the COP of the system is clearly improved when the evaporator operates at 10.5 °C (which corresponds to a cold source temperature at 15.5 ° C) rather than 0.5°C (which corresponds to a cold source at 5.5 °C). For η_e = 0.5, the COP increases up to 1.2 when the condenser operates at 20 °C and decreases down at 0.2 when the condenser operates at 40° C. For η_e =0.7, the COP is 0.3 when the condenser operates at 40 °C, and we can observe for other condenser temperature values that the performance of the system is significantly improved. In this case, the maximum COP reaches 1.8 when the temperature difference between the condenser (30°C) and the evaporator (10,5°C) is drastically reduced to 9.5 °C.

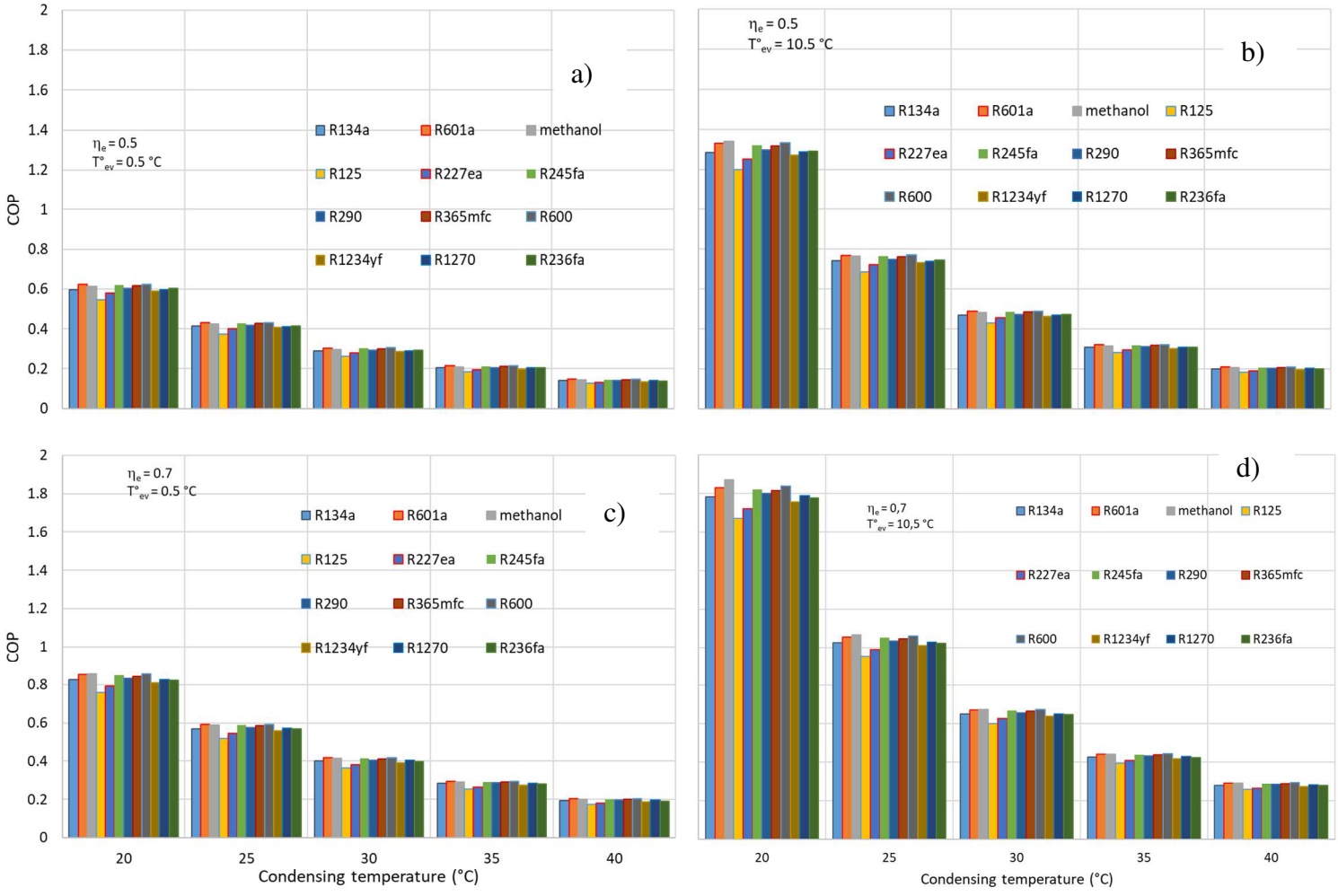

Fig. 2. Coefficient of performance

The choice of fluid shows only a slight possibility to improve the COP. A similar result was reported by Nasir and Kim (2016) which recommends looking at other criteria such as the pressure ratio to classify the fluids. Here, the COP is reduced by 50% when the condensation temperature increases from 30 to 40°C. Conversely, the COP is increased (+ 100%) when the condensing temperature goes from 30 to 20°C. When the condensation temperature drops, the effect is positive for the ORC cycle because the thermal contrast between the hot and cold sources is increased. In practice, this leads to a higher-pressure ratio between the inlet and the outlet of the expander leading to increase the specific work produced. At the same time, the temperature drop of the condenser decreases the pressure ratio of the compressor, which causes a reduction in the specific work required. Thus, the compressor benefit from more power that allow to carry a higher flow. It is then best to lower the condensing temperature by improving the condenser design rather than choosing another fluid. Nasir's results indicate a slight increase in COP as the condenser temperature increases. This difference is mainly explainable by using separate cycles / common condenser cycle. It can also be noted that the classification of fluids according to their COP does not correspond to the classification of fluids according to the entrainment ratio. This result can be explained because the fluid is either more suitable for the ORC cycle, or more suitable for the VCC cycle, but not for both applications simultaneously. Thus, the fluids giving a good driving efficiency lead to a low cooling effect and, conversely, the fluids giving a poor engine efficiency give a good effect of refrigeration. This behavior is due to the inclination of the isentropic lines in the vapor section of the P, H diagram. When the isentropic slope is low, work is high. This favors the motor effect of ORC cycle but disadvantages the VCC performance as it increases the required specific work of the compressor.

3.2. Required volumetric ratios

Fig. 3 represents the volumetric expansion ratio (V5/V4) as a function of the volumetric compression ratio (V12/V6) for all the fluids, when η_e =0.5 and T_{ev} = 0.5°C. This figure contains two sectors marked A and B. Zone A corresponds to the situations for which the expansion ratio is higher than the compression ratio. Conversely, sector B corresponds to the cases for which the compression ratio is greater than the expansion ratio. The dotted line corresponds to the particular case for which the two ratios are equal.

When the condensing temperature is low (20 and 25°C), the expansion ratio is always higher than the compression ratio for all fluids. Inversely, when the condenser temperature exceeds 30°C, the volumetric expansion ratio is smaller than the compression ratio.

Finally, we observed that the choice of the fluid strongly changes the value of the compression ratio and the expansion ratio. The minimum compression or expansion ratio are close to 2.0, while the highest ones are 5.5. Fig. 4 shows the ratio of small diameters (compressor outlet / expender inlet) against the ratio of large diameters (compressor inlet / expander outlet), for η_e=0,5 and T_{ev} = 0,5°C.

In this figure, the iso-ratio lines are also represented in dotted lines. They mark the situations for which the volume flows, and therefore the corresponding required diameters at the inlet / outlet of the compressor and expander are equal. The four sectors, C, D, E and F mark the situations for which diameters must be different. For example, sector F corresponds to cases where the compressor input D_{12} is larger than the expander output D_5 (V12> V5) and the compressor output D_6 is smaller than the expander input D_4 (V6 <V4).

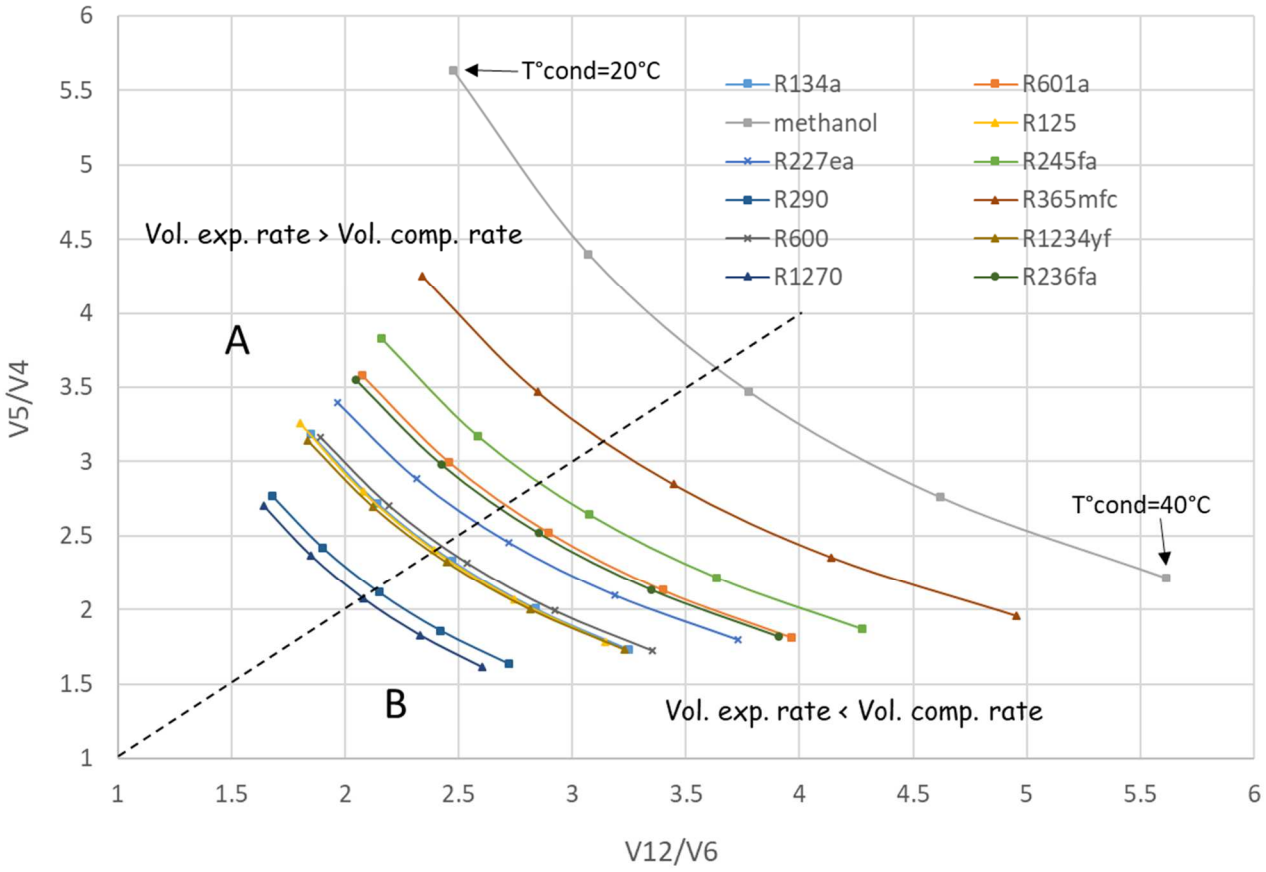

Fig. 3. Compressor-expender volumetric ratios with η_e=0,5 and T_{ev} = 0,5°C.

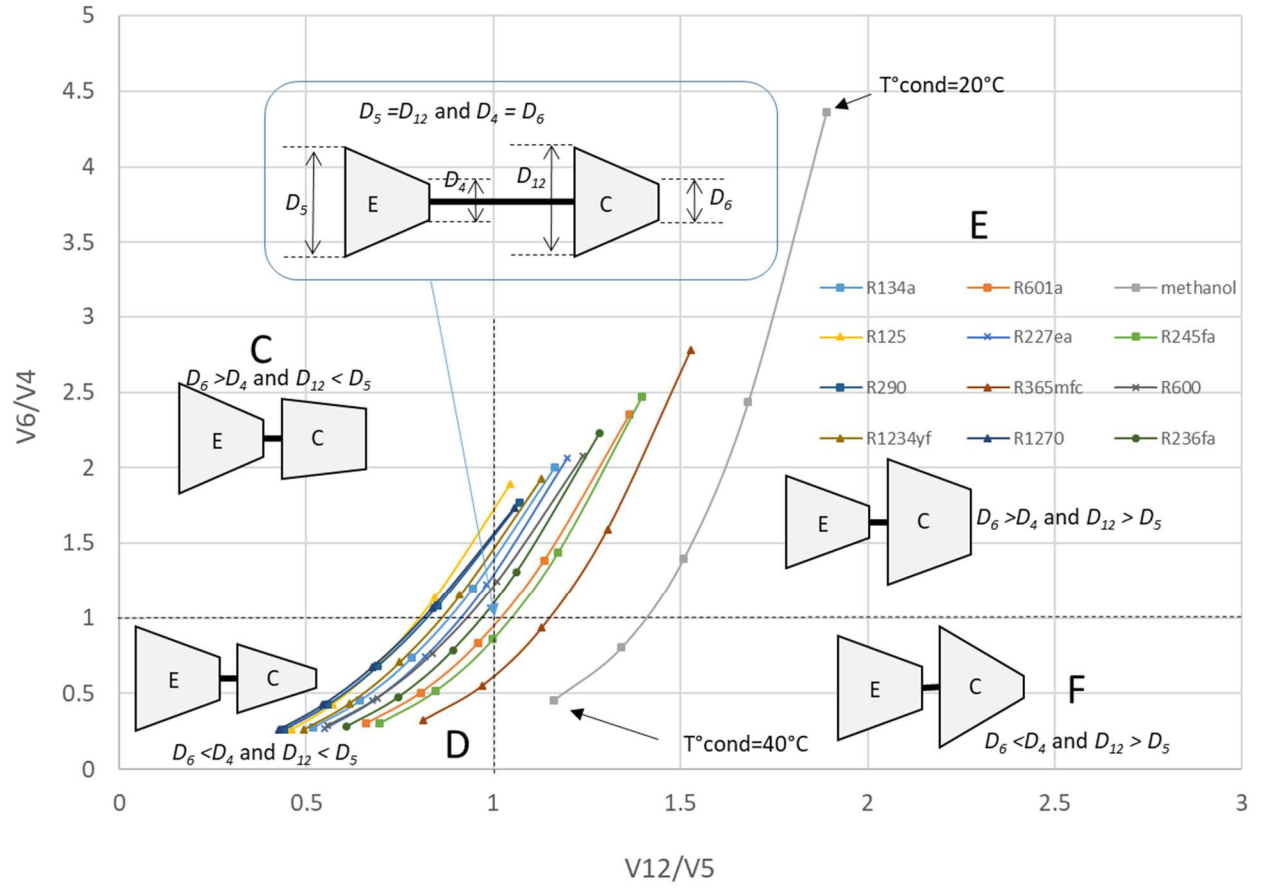

Fig. 4. Small orifice c-e ratio vs large orifice c-e ratio, with η_e= 0,5 and T_{ev} = 0,5°C.

Changing the temperature of the condenser causes the operating point to move in the three sectors D; C; E for almost all fluids. The operating point passes through sectors D; F; E for R601a, R245fa, and R365mfc. Finally, only E and F sectors are possible for methanol. It appears in this figure that the fluids are classified according to their boiling point. R125, having the lowest boiling point, is the furthest left, while methanol, which has the highest boiling point, is rightmost. When the system contains R601a and the condensation temperature is 30 °C, the small diameters D_4 and D_6 are equal and the large diameters D_5 and D_{12} are equal.

As confirmed in Fig. 4, the expansion ratio then coincides with the compression ratio for this particular case. The compressor therefore has exactly the same geometrical characteristics than the expander, which makes it possible to use two identical volumetric compressors, one of which is used as an expender.

The effect of the evaporation temperature is studied by renewing the same calculations for T_{ev} = 10.5 ° C. Fig. 5 represents the volumetric expansion ratio as a function of the volumetric compression ratio for all the fluids, for this new temperature. Comparing with Fig. 3, there is a marked decrease in the abscissae of the points tested leading to a displacement of the points on the side of the sector A. The use of this system for T_{ev} = 10.5 °C therefore imposes volumetric ratios generally greater than compression volumetric ratios. Only the installations for which the condensing temperature will be greater than approximately 35° C required the volumetric expansion ratios being lower than compression volumetric ratios.

Fig. 6 represents the ratios of the volumetric flow rates for the small diameters (D_6 and D_4) , as a function of the ratio of the large diameters (D_{12} and D_5), for T °$_{ev}$ = 10.5 ° C. The behavior already observed in Fig. 4 is preserved but there is a strong spread of points vertically. This time, the possibility of using similar expander and compressor is obtained with the R365mfc, when the operating temperature of the condenser is 33 °C.

The results clearly show the influence of the operating conditions on the dimensional characteristics at the inlet/outlet of the expander and at the outlet / inlet of the compressor. The effects are observed for the volumetric flow rates, the compression and expansion ratios. Again, it is possible to obtain operating conditions for which the geometrical characteristics of the expander are exactly the same as those of the compressor.

When one wants to design a small-scale prototype, one solution is to use a compressor as an expander. Volumetric compressors such as scrolls seem particularly appropriate. However, the choice of the compressor that will run as an expander must have the good volumetric expansion ratio and must be correctly fitted to the volume flow that must be transformed. The choice of the compressor is usually established according to a nominal working point. When the system must operate outside the nominal point, the risk of over/ under compression over/under expansion exists. Figures presented here allow evaluating the risk of operation with an over or under compression / expansion as they allow direct viewing of the distance between a nominal point and a current working point.

The initial value of the efficiency of the expander is η_e=0,5. This value is particularly low and corresponds to the efficiency measured experimentally on a non-optimized micro expander (Marion and Louahlia, 2017). One can expect that the more appropriate design of the expander should improve its performance. The effect of the expander efficiency improvement is studied by renewing the same calculations with η_e=0,7.

3.3. Impact of expander efficiency

By comparing the results of Fig. 7 with those of Fig. 4, it appears that increasing the efficiency of the expander from 0.5 to 0.7 moves all the points to the right. No more operating points pass through sector C. The same effect is observed between Fig. 6 and 8. In Fig. 7, the particular operating mode when $D_{12} = D_5$ and $D_6 = D_4$, corresponding to the case when the compressor and the expander are identical is obtained for R125, R290 and R1270 when the condensation temperature is close to 30. In Fig. 8, the same situation is obtained for R134a, R227ea and R1234yf for similar temperature of condensation.

Table 2 shows all the identified particular cases for which the compressor can be identical to the expander. The compression / expansion volumetric ratios and the inlet and outlet diameters of the compressor or expander were reported.

Table 2
Special cases for which compressor and the expander are identical

T°ev	0.5 °C	10.5 °C	0.7 °C	0.7 °C	0.7 °C	0.5 °C	0.5 °C	0.5 °C
η_e	0.5	0.5	0.5	0.5	0.5	0.5	0.5	0,5
fluid	R601a	R365mfc	R125	R1270	R290	R134a	R227ea	R1234yf
T° cond (°C)	28	33.6	30	30	29.5	34.5	34	34.5
V5/V4 ; V12/V6	2.7	2.5	2.37	2.04	2.1	2.02	2.15	2.01
D12 ; D5 (mm)	22.4	23.5	6.6	7.4	8.1	8.4	10	8.6
D4 ; D6 (mm)	13.5	14.8	4.3	5.1	5.6	5.9	6.9	6

Among the particular cases studied here, the volumetric ratios of compression or expansion vary from 2.01 to 2.7. This corresponds to a small amplitude compared to the ratios observed in Fig. 3 and Fig. 5. Large diameters range from 23.5 mm to 6.6 mm while small diameters range from 4.3 mm to 14.8 mm. This high range shows that the size of the compressor and the expander are highly dependent on the choice of fluid. The required condensation temperature varies from 28°C to 34.5°C. These particular cases are therefore recommended to designers wishing to achieve simply an ORC-VCC system from two identical volumetric compressors, one operating as an expander.

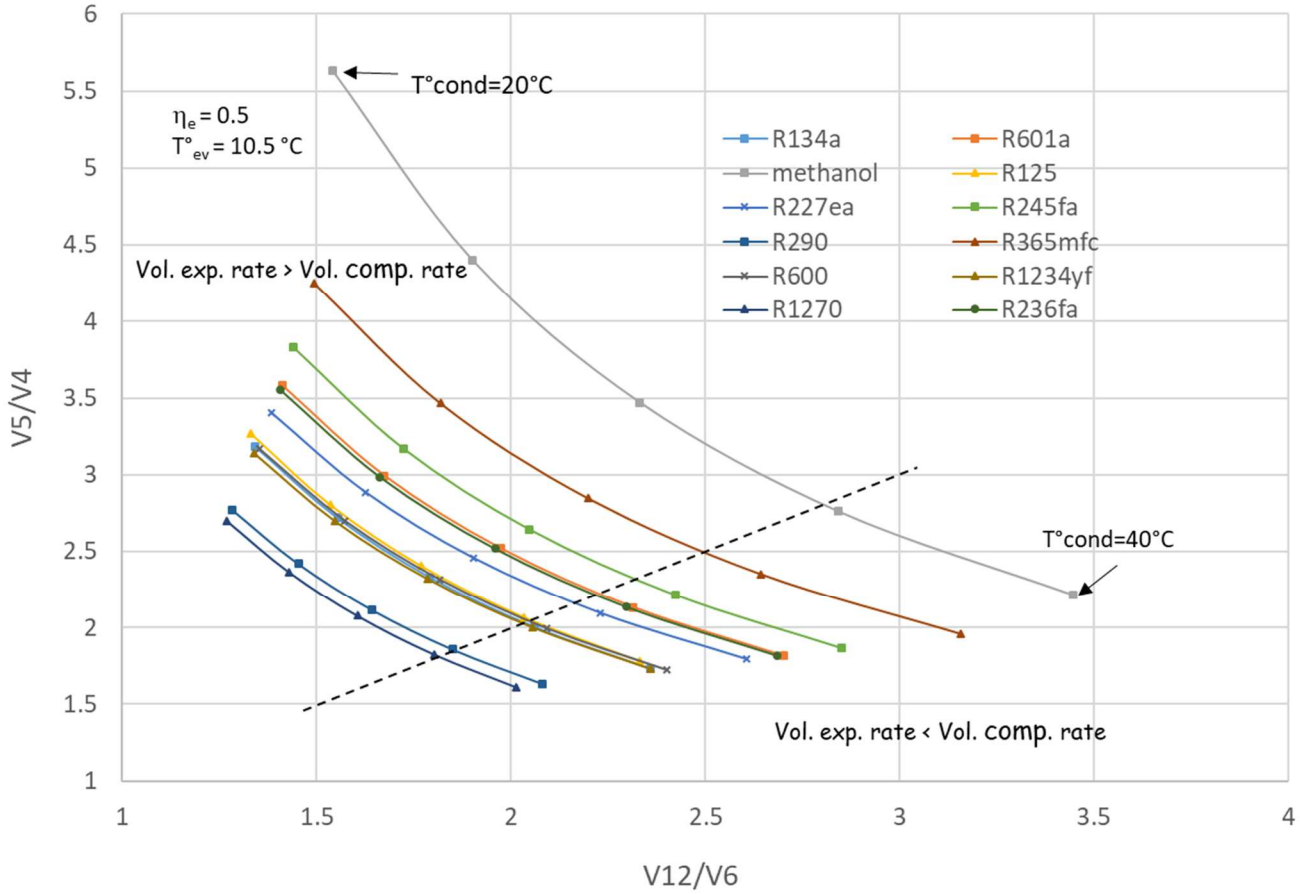

Fig. 5. Compressor-expender volumetric ratios with η_e=0.5 and T_{ev} = 10.5°C.

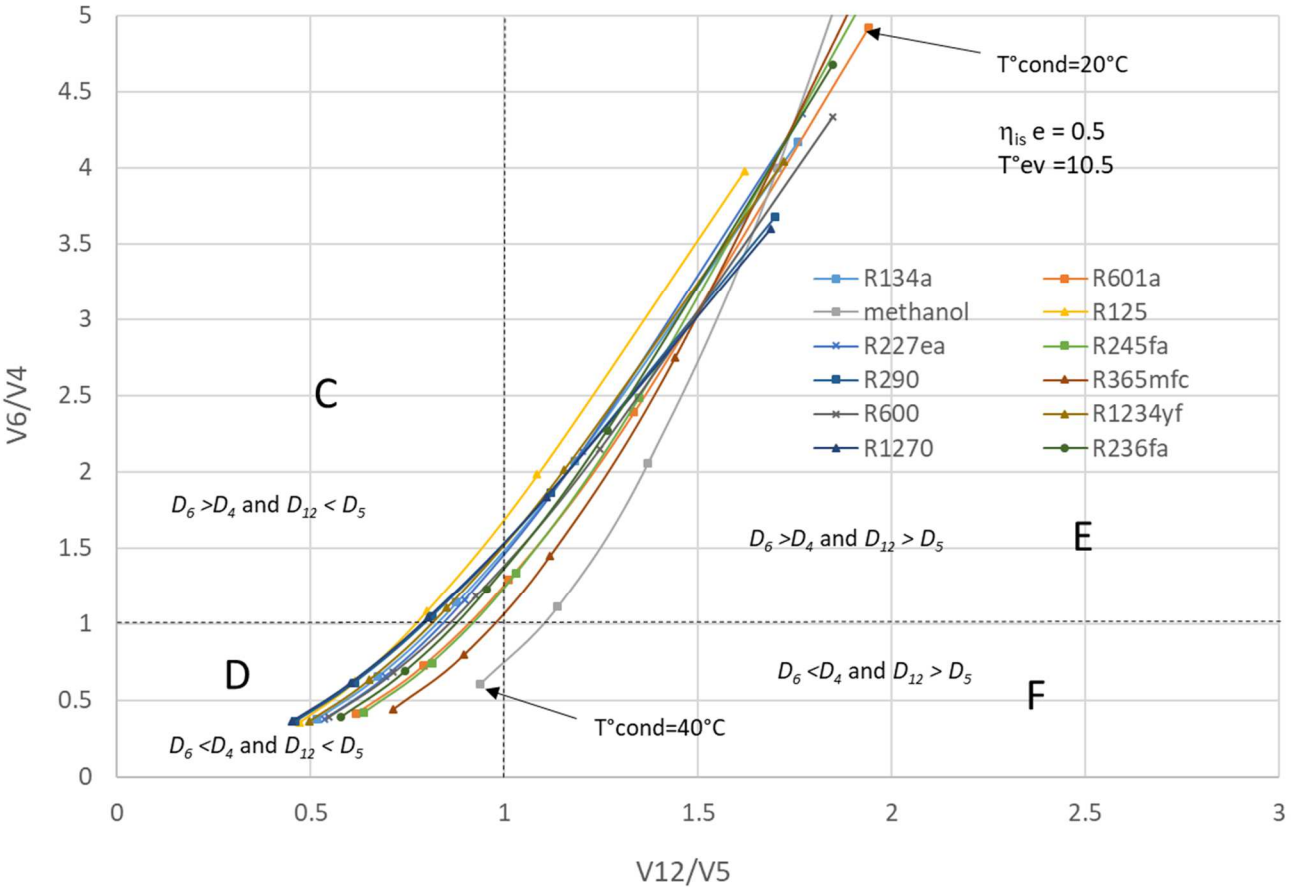

Fig. 6. Small orifice c-e ratio vs large orifice c-e ratio with η_e=0.5 and T_{ev} = 10.5°C.

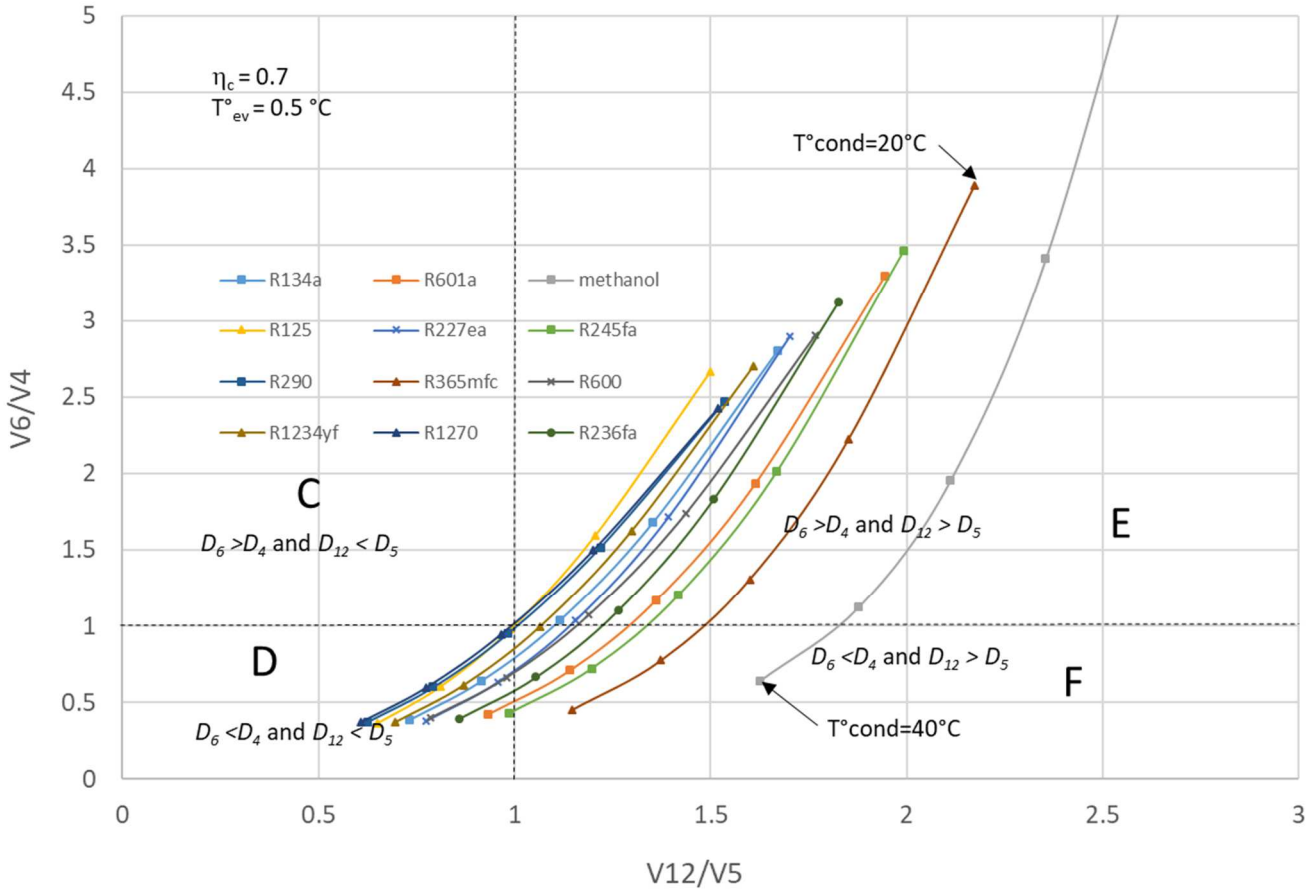

Fig. 7. Small orifice c-e ratio vs large orifice c-e ratio, η_e=0.7 and T_{ev} = 0.5°C.

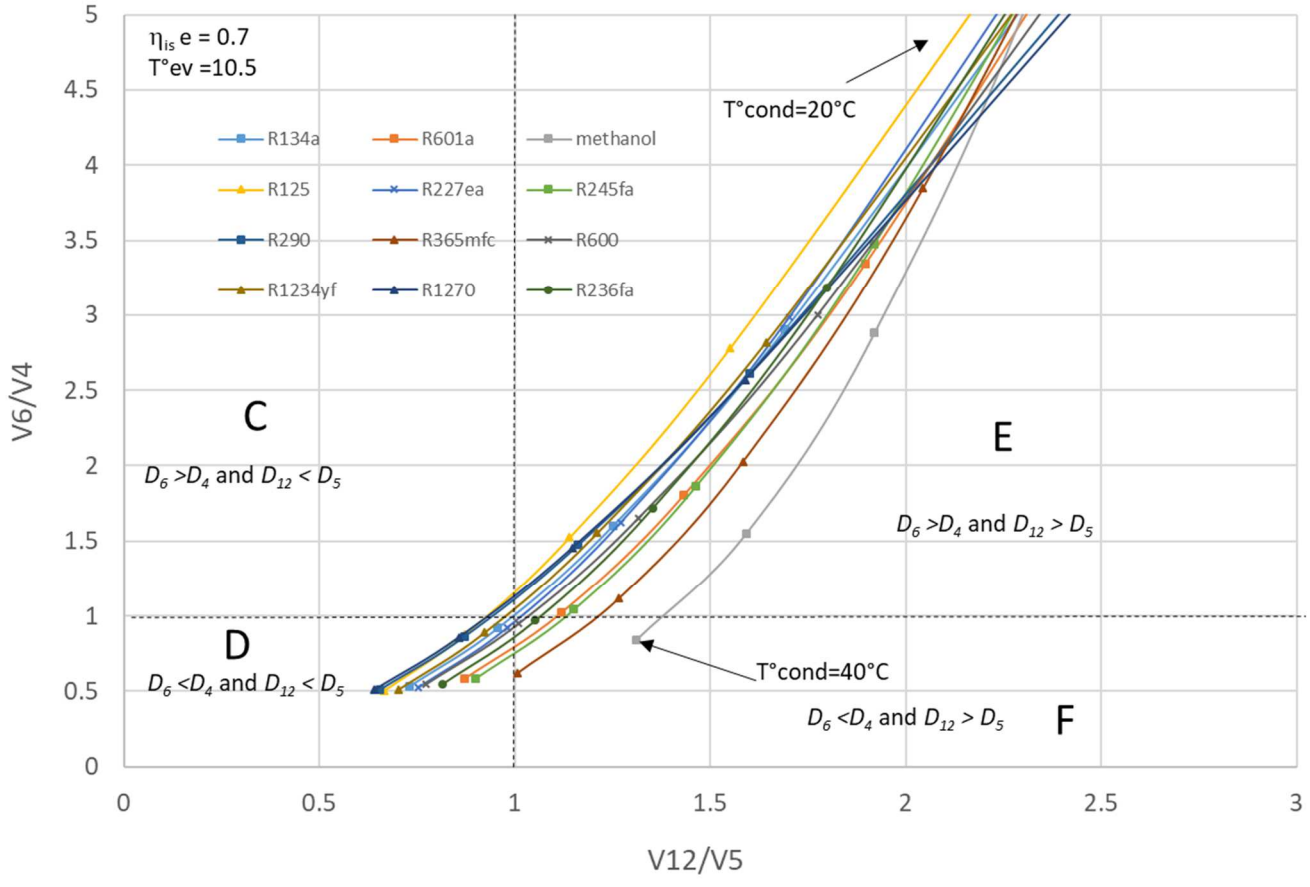

Fig. 8. Small orifice c-e ratio vs large orifice c-e ratio, η_e=0.7 and T_{ev} = 10.5°C.

4 Conclusion

The study of an ORC cycle (engine) combined with a VCC cycle (cooler) with a common condenser and working with the same fluid is studied. The thermodynamic transformations from one point to the other of the system are modeled by a one-dimensional approach that considers the pressure losses in the various sections of the system as well as the isentropic efficiencies of the compressor, the expander and the pump. A parametric study focused on the temperature of the condenser and the temperature of the evaporator is conducted. For all the cases studied here, the heating source power was 2 kW at 65 °C. Twelve organic fluids commonly used for mechanical compression refrigeration machines or for ORC systems were tested. The results give the required diameters ratios at the inputs and outputs of the compressor and the expender. For all the cases studied, all the possible combinations ($D_5 < D_{12}$ and $D_4 < D_6$; $D_5 > D_{12}$ and $D_4 < D_6$; $D_5 < D_{12}$ and $D_4 > D_6$; $D_5 > D_{12}$ and $D_4 > D_6$) were encountered. Even a moderate change in condenser temperature can move the system from one configuration to another. In some particular cases, we can observe $D_4 = D_6$ and $D_5 = D_{12}$, corresponding to the case where the compressor and the expander orifice diameters are identical. The identification of dimensional constraints at the compressor and expander inlets and outlets obtained here will allow developers or users of this type of system to reduce the risk of operation with over / under compression / expansion. The system can thus produce a useful cooling capacity of 0.60 kW when the cold source temperature is 5.5 ° C and when the condenser temperature is 30 °C. The cooling capacity reaches 1.0 kW if the cold source temperature is 15.5 °C.

References

Aphornratana, S., Sriveerakul, T., 2010. Analysis of a combined Rankine–vapour–compression refrigeration cycle. Energy Conv. and Manag. 51, 2557–2564. http://dx.doi.org/10.1016/j.enconman.2010.04.016.

Bao, J., Zhang, L., Song, C., Zhang, N., Zhang, X., He, G., 2020. Comparative study of combined organic Rankine cycle and vapor compression cycle for refrigeration: Single fluid or dual fluid? , Sustainable Energy Technologies and Assessments 37 , 1005095. https://doi.org/10.1016/j.seta.2019.100595.

Bracco, R., Clemente, S., Micheli, D., Reini, M., 2015. Experimental tests and modelization of a domestic-scale ORC (Organic Rankine Cycle). Energy, 58, 107–116. http://dx.doi.org/10.1016/j.energy.2012.12.016.

Chang, H., Wan, Z., Zheng, Y., Chen, X., Shu, S., Tu, Z., Hwa Chan, S., 2017. Energy analysis of a hybrid PEMFC–solar energy residential micro-CCHP system combined with an organic Rankine cycle and vapor compression cycle. Energy Conv. and Manag. 142, 374–384. http://dx.doi.org/10.1016/j.enconman.2017.03.057.

Demierre, J., Favrat, D., Schiffmann, J., Wegele, J., 2014. Experimental investigation of a Thermally Driven Heat Pump based on a double Organic Rankine Cycle and an oil-free Compressor-Turbine Unit. Int. J. Refrigeration, 44, 91–100. http://dx.doi.org/10.1016/j.ijrefrig.2014.04.024.

Eames, I.W., Milazzo, A., Paganini, D., Livi, M., 2013. The design, manufacture and testing of a jet-pump chiller for air conditioning and industrial application. Appl. Therm. Eng. 58, 234-240. http://dx.doi.org/10.1016/j.applthermaleng.2013.04.028.

Habibzadeh, A., Rashidi, M. M., Galanis, N., 2013. Analysis of a combined power and ejector-refrigeration cycle using low temperature heat. Energy Conv. and Manag. 65, 381–391. http://dx.doi.org/10.1016/j.enconman.2012.08.020.

Karellas, S., Braimakis, K., 2016. Energy–exergy analysis and economic investigation of a cogeneration and trigeneration ORC–VCC hybrid system utilizing biomass fuel and solar power. Energy Conv. and Manag. 107, 103–113. http://dx.doi.org/10.1016/j.enconman.2015.06.080.

Jeong, J. Kang, Y.T., 2004. Analysis of a refrigeration cycle driven by refrigerant steam turbine, Int. J. Refrigeration. 27, 33–41. doi:10.1016/S0140-7007(03)00101-4

Kim, K. H., Perez-Blanco, H., 2015. Performance analysis of a combined organic Rankine cycle and vapor compression cycle for power and refrigeration cogeneration. Appl. Therm. Eng. 91, 964-974. http://dx.doi.org/10.1016/j.applthermaleng.2015.04.062.

Li, H., Bu, X., Wang, L., Long, L., Lian, Y., 2013. Hydrocarbon working fluids for a Rankine cycle powered vapor compression refrigeration system using low-grade thermal energy. Energy and Build. 65, 167–172. http://dx.doi.org/10.1016/j.enbuild.2013.06.012.

Li, L., Ge, Y. T., Luo, X., Tassou, S. A., 2017. Experimental investigations into power generation with low grade waste heat and R245fa Organic Rankine Cycles (ORCs). Appl. Therm. Eng. 115, 815–824. http://dx.doi.org/10.1016/j.applthermaleng.2017.01.024.

Lizarte, R., Palacios-Lorenzo, M. E., Marcos, J. D., 2017. Parametric study of a novel organic Rankine cycle combined with a cascade refrigeration cycle (ORC-CRS) using natural refrigerants. Appl. Therm. Eng., 127, 378–389. http://dx.doi.org/10.1016/j.applthermaleng.2017.08.063.

Marion, M., Louahlia, H., 2017. “Performances and compactness of a cooling system powered with PEMFC thermal effluent”, Energy Conv. and Manag, 150, 415–424. http://dx.doi.org/10.1016/j.enconman.2017.07.066.

Mazzelli, F., Milazzo, A., 2015. Performance analysis of a supersonic ejector cycle working with R245fa. Int. J. Refrigeration. 46, 79-92. http://dx.doi.org/10.1016/j.ijrefrig.2014.09.020.

Molés, F., Navarro-Esbrí, J., Peris, B., Mota-Babiloni, A., Kontomaris, K., 2015. Thermodynamic analysis of a combined organic Rankine cycle and vapor compression cycle system activated with low temperature heat sources using low GWP fluids. Appl. Therm. Eng. 87, 444-453. http://dx.doi.org/10.1016/j.applthermaleng.2015.04.083.

Muhammad, U., Imran, M., Lee,D. H., Park, B. S., 2015. Design and experimental investigation of a 1 kW organic Rankine cycle system using R245fa as working fluid for low-grade waste heat recovery from steam. Energy Conv. and Manag. 103, 1089–1100. http://dx.doi.org/10.1016/j.enconman.2015.07.045.

Nasir, M. T., Kim, K. C., 2016. Working fluids selection and parametric optimization of an OrganicRankine Cycle coupled Vapor Compression Cycle (ORC-VCC) for air conditioning using low grade heat. Energy and Build. 129, 378–385. http://dx.doi.org/10.1016/j.enbuild.2016.07.06.

Nasir M. T., Ali M. A., Khan T. S., Al-Hajri E., Kadri M. B., Kim K. C., 2019. Performance assessment and multi objective optimization of an Organic Rankine Cycle driven cooling air conditioning system. Energy and Buildings 191, 13-30. https://doi.org/10.1016/j.enbuild.2019.03.012.

NIST Standard Reference Database 23, 2010. Thermodynamic and Transport Properties of Refrigerant and Refrigerant Mixtures REFPROP, Version 9.0.

Pu, W., Yue, C., Han, D., He, W., Liu, X., Zhang, Q., Chen, Y., 2016. Experimental study on Organic Rankine cycle for low grade thermal energy recovery. Appl. Therm. Eng. 94, 221–227. http://dx.doi.org/10.1016/j.applthermaleng.2015.09.120.

Quoilin, S., Lemort, V., Lebrun, J., 2010. Experimental study and modeling of an Organic Rankine Cycle using scroll expender. Appl. Energy, 87, 1260-1268. http://dx.doi.org/10.1016/j.apenergy.2009.06.026.

Saleh, B., 2016. Parametric and working fluid analysis of a combined organic Rankine-vapor compression refrigeration system activated by low-grade thermal energy. Journ. of Adv. Research, 7, 651–660. http://dx.doi.org/10.1016/j.jare.2016.06.006.

Tchanche, B.F., Papadakis, G., Lambrinos, G., Frangoudakis, A. 2009. Fluid selection for a low temperature solar organic Rankine cycle. Appl. Therm. Eng. 29, 2468-2476. doi:10.1016/j.applthermaleng.2008.12.025.

Wang, H., Peterson, R., Harada, K., Miller, E., Ingram-Goble, R., Fisher, L., Yih, J., Ward, C., 2011. Performance of a combined organic Rankine cycle and vapor compression cycle for heat activated cooling. Energy, 36, 447-458. doi:10.1016/j.energy.2010.10.020.

Wang, H., Cai, W., Wang, Y., Yan, J., Wang, L., 2016. Experimental study of the behavior of a hybrid ejector-based air-conditionning system with R134a, Energy Conv. and Manag. 112, 31-40. http://dx.doi.org/10.1016/j.enconman.2016.01.010.

Wang, Z. X., Li, H. Y., Zhang, X. F., Wang L. W., Du S., Fang, C., 2020. Performance analysis on a novel micro- scale combined cooling, heating and power (CCHP) system for domestic utilization driven by biomass energy, Renew. Energy 156, 1215-1232. https://doi.org/10.1016/j.renene.2020.04.108.

Wu, D., Aye, L., Ngo, T., Mendis, P., 2017. Optimisation and financial analysis of an organic Rankine cycle cooling system driven by facade integrated solar collectors. Appl. Energy, 185, 172–182. http://dx.doi.org/10.1016/j.apenergy.2016.10.071.

Yilmaz, A., 2015. Transcritical organic Rankine vapor compression refrigeration system for intercity bus air-conditioning using engine exhaust heat. Energy, 82, 1047-1056. http://dx.doi.org/10.1016/j.energy.2015.02.004.

Yue, C., You, F., Huang, Y., 2016. Thermal and economic analysis of an energy system of an ORC coupled with vehicle air conditioning. Int. J. Refrigeration, 64, 152–167. http://dx.doi.org/10.1016/j.ijrefrig.2016.01.005.

Zeyghami, M., Goswami, D. Y., Stefanakos, E., 2015. A review of solar thermo-mechanical refrigeration and cooling methods. Renew. Sustain. Energy Rev. 51, 1428–1445. http://dx.doi.org/10.1016/j.rser.2015.07.011.

Zheng, N., Wei, J., Zhao, L., 2018. Analysis of a solar Rankine cycle powered refrigerator with zeotropic mixtures. Solar Energy, 162, 57–66. https://doi.org/10.1016/j.solener.2018.01.011.

Appendix : Thermodynamic model

Present ORC-VCC system is simulated using one-dimensional steady-state flow model. Fluid properties are calculated for each point identified in Fig. 1 using the NIST REFPROP software and the following equations.

Enthalpy balance:

in the pump:

$$H_2 = H_1 + \frac{H_{2is} - H_1}{\eta_p} \tag{1}$$

in pressure reducing valve:

$$H_{11} = H_{10} \tag{2}$$

in the preheater:

$$H_3 = H_2 + \eta_g (H_{3\max} - H_2) \tag{3}$$

Where $H_{3\max}$ is calculated at P_3 and T_7.

in the expender:

$$H_5 = H_4 + \eta_e (H_{5is} - H_4) \tag{4}$$

in the compressor:

$$H_6 = H_{12} + \frac{(H_{6is} - H_{12})}{\eta_c} \tag{5}$$

mixing fluids at point 7:

$$H_7 = \frac{\dot{m}_p H_5 + \dot{m}_s H_6}{\dot{m}_p + \dot{m}_s} \tag{6}$$

Power:

Pump:

$$\dot{W}_p = \dot{m}_p (H_2 - H_1) \tag{7}$$

Evaporator

$$\dot{Q}_{ev} = \dot{m}_s (H_{12} - H_{11}) \tag{8}$$

Generator:

$$\dot{Q}_{gen} = \dot{m}_p (H_4 - H_3) \tag{9}$$

Preheater:

$$\dot{Q}_{pre} = \dot{m_p}(H_3 - H_2) = (\dot{m}_p + \dot{m}_s)(H_7 - H_8) \tag{10}$$

Condenser:

$$\dot{Q}_{cond} = (\dot{m}_p + \dot{m}_s)(H_9 - H_{10}) \tag{11}$$

expander:

$$\dot{W}_e = \dot{m}_p (H_4 - H_5) \tag{12}$$

Compressor

$$\dot{W}_c = \dot{m}_s (H_6 - H_{12}) \tag{13}$$

Considering additional mechanical friction between expander and compressor:

$$\dot{W}_c = \eta_m \dot{W}_e \tag{14}$$

Hydraulic diameters are calculated at each point i, using:

$$D_i = \sqrt{\frac{4\dot{m}_i}{\pi \rho_i v_i}} \tag{15}$$

Pressure losses between two consecutive points i and j are calculated from the Darcy-Weisbach equation:

$$\Delta P_{ij} = \Lambda_{ij} \frac{8 L_{ij}}{\pi^2 D_i^5 \rho_i} \dot{m}_i^2 \tag{16}$$

For Reynolds numbers ranging from 4,000 to 100,000, one can use the Blasius correlation:

$$\Lambda_{ij} = 0.3164 \mathrm{Re}_{ij}^{-0.25} \tag{17}$$

For smaller Reynolds numbers, we used

$$\Lambda_{ij} = 64 \mathrm{Re}_{ij}^{-1} \tag{18}$$

Reynolds number in any section ij has been calculated using the mean values of fluid properties at the input and output of the section.